



Fermi National Accelerator Laboratory

FERMILAB-Pub-96/126

Position Resolution of MSGCs with Cathode Readout

N. Amos et al.

*Fermi National Accelerator Laboratory
P.O. Box 500, Batavia, Illinois 60510*

June 1996

Submitted to *Nuclear Instruments and Methods*

Disclaimer

This report was prepared as an account of work sponsored by an agency of the United States Government. Neither the United States Government nor any agency thereof, nor any of their employees, makes any warranty, expressed or implied, or assumes any legal liability or responsibility for the accuracy, completeness, or usefulness of any information, apparatus, product, or process disclosed, or represents that its use would not infringe privately owned rights. Reference herein to any specific commercial product, process, or service by trade name, trademark, manufacturer, or otherwise, does not necessarily constitute or imply its endorsement, recommendation, or favoring by the United States Government or any agency thereof. The views and opinions of authors expressed herein do not necessarily state or reflect those of the United States Government or any agency thereof.

Position Resolution of MSGCs with Cathode Readout

N. Amos^b, L. Cremaldi^d, G. Finocchiaro^g, B. Gobbi^c, K.K. Ng^g,
V. Manzella^g, V. Peskov^c, S. Rajagopalan^g, P. Rubinov^c, D. Schamberger^g,
G. Sellberg^a, J. Steffen^g, R. Tilden^c, P. Wang^e, Y. Yu^f

^a*Fermi National Accelerator Laboratory, Batavia, IL 60510*

^b*University of Michigan, Ann Arbor, MI 48109*

^c*Northwestern University, Evanston, IL 60208*

^d*University of Mississippi, University, MS 38677*

^e*Purdue University, Lafayette, IN 47907*

^f*Seoul National University, Seoul, Korea*

^g*State University of New York, Stony Brook, NY 11794*

(June 3, 1996)

The performance of a telescope of Micro-Strip Gas Chambers (MSGC) has been studied in a beam of pions. Detectors with different anode pitch and with different substrates have been operated using several gas mixtures. The position resolutions obtained by reading out the cathodes for the 200 μm pitch is 42 μm . For the 400 μm pitch detectors the resolution is 42 μm after correcting the centroid positions with a function derived from the data.

I. Introduction

Micro-Strip Gas Chambers were first proposed by A. Oed [1]. Their key component is the substrate, a resistive layer with a pattern of narrow parallel electrodes printed using techniques developed for the microelectronics industry. They operate reliably up to high rates ($10^6 \text{mm}^{-2} \text{sec}^{-1}$) and give excellent position resolution ($\sim 40 \mu\text{m}$) for tracks at normal incidence. The requirements for tracking detectors that will operate at the next generation of accelerators are well satisfied by MSGCs. Extensive studies of these detectors have been carried out in the laboratory [2] – [5] and in test beams [6] – [12] although their use in experiments has been limited. [13], [14] The CMS [15] experiment at the LHC is committed to use a system of over 10 million channels of MSGCs for tracking outside the pixels and silicon microstrip detectors. Parameters that have received considerable attention in the study of MSGCs include the position resolution and its angular dependence as well as the ability to identify two closely spaced MIPs. The signal amplitude and the aging of the detector have been studied for different gas mixture. Less attention has been given to the performance of MSGCs when the pitch of the detector is changed. We are presenting here the performance of chambers with a 400 μm as well as the

conventional 200 μm pitch tested with 8 different gas mixtures of DME with Ar or Ne.

II. Experimental Setup

A. The Beam

The beam test was carried out with four MSGC units at a time. Three scintillation counters in coincidence defined the trigger. No external tracking telescope was available. The gas for the chambers was supplied by an open type system and the mixing was controlled with mass flowmeters; this system does not conform with clean gas system criteria [16]. Each MSGC was mounted on an aluminum frame, which was installed on an aluminum reference table (Figure 1) with special attention placed on avoiding relative rotations of the substrates. This test was carried out in a test beam using a 5 GeV/c pion beam at the AGS at Brookhaven National Laboratory during the first half of 1995. The beam had a divergence of a few mrad with incidence perpendicular to the detectors, with electrodes positioned horizontally. Beam rates through the telescope were 10 to 50 kHz and the data were recorded at 10 Hz by a CAMAC based data acquisition system. About 10 million triggers were logged during this test.

B. Detectors

The detectors are built on $10 \times 10 \text{ cm}^2$ substrates of Desag D-263 or Schott S-8900 glass plates of 0.3 and 7 mm thick respectively [17]. The sensitive area covers $32 \times 64 \text{ mm}^2$ equally subdivided into a region with 80 electrodes, separated by 200 μm , and a region of 40 electrodes with a pitch of 400 μm . The anode width is 10 μm and the anode-cathode gap is 60 μm . The anodes are connected on the substrate in 10 groups of 8 and 4 for the 200 and 400 μm pitch regions respectively. Anode groups and individual cathodes are then fanned out and extended to the periphery of the substrate for easy connections to the electronics. A gas volume, 3 mm high, is defined by a Noril spacer and a drift electrode made of a plastic window with transparent conductive coating. The gas seal is made with an O-ring. The same aluminum frame on which the MSGC is mounted, also positions the electronics board relative to the substrate, one board at each end of the electrodes. Connections between detector and electronics boards are made by elastomer connectors [18] (rather than microbonding), which allow either substrate or electronics boards to be replaced quickly. The modular design facilitates the testing of different configurations.

C. Readout Electronics

The board distributing the HV also carries two hybrid 8-channel preamplifiers [19] and a 150 pF decoupling capacitors for each channel, to read out groups of anodes (more detail can be found in ref. [12]). The cathodes are kept at ground potential and read out by 4 hybrids using Fujitsu common base preamplifiers, totaling 32 channels. The 32 channels can record the information of 120 cathodes because each channel reads 4 cathodes which are separated by 30 cathodes. Ambiguities are resolved using the information of the anodes so that the hit position is uniquely determined. The absolute gain of the readout system is measured by injecting, with a pulser, a calibration charge on a capacitor located at the input of each preamplifier channel. From the preamplifiers, the signals are transported 30 m with a coaxial cable to shaper-amplifier boards and after another 30 m of cables they are digitized with CAMAC ADCs (LRS 2229A). Each of the four chambers has 48 readout channels for a total of 192 ADC channels. The gate to the ADCs was set to 75 ns. The noise of the readout system has been measured to be about 5000 electrons equivalent r.m.s., and the gain to be approximately 1100 electrons per ADC count. The linearity of the system, measured with the test pulse, was better than 2%.

III. Analysis and Results

The cathodes measure the charge distribution generated by an avalanche in the MSGCs. This information is used to form a cluster which is defined as a sequence of one or more cathode channels with content greater than three sigma above the pedestal value of the same channel. The content of the ADC has been corrected for channel to channel gain variations in the read out chain. The distribution of cluster multiplicity from the data for MIP particles through the 200 and 400 μm regions are given in Figure 2. In the following, we call the hit the center of mass (centroid) which we assume, to first approximation, represent the position of the track. We define tracks as events with three chamber hits along a straight line.

A. Efficiencies

The efficiency of a MSGC for detecting a MIP has been measured as a function of the HV by taking the fraction of events that have a hit in the chamber under test when there are hits consistent with a track formed using the outer two chambers. The results are summarized in Figure 3a) for the region with

200 μm pitch, and the 400 μm first in b) for mixtures of Ar/DME, and second in c) of Ne/DME. These measurements were done using the information of the anodes. One can observe the same signal on a 200 μm chamber as a 400 μm one by raising the HV by 100 V. Results using a gas mixture with Ne/DME have been recently reported in the literature [5], [12].

B. Landau Distributions

Figure 4a) through d) give a direct comparison of the signal amplitude recorded by reading out the information from both the anodes and cathodes of MSGCs with a 200 and 400 μm pitch. The figures show both pedestal and cluster distribution for chambers operated with 100% DME. The value of the most probable and of the average charge deposited is shown in units of signal to noise (S/N). Recently there is interest in using Ne rather than Ar because of the possibility that Ne reduces and possibly eliminates aging [20]. Figure 5a) through d) shows the signal distributions measured with the anodes of a 400 μm pitch MSGC for different Ne content of the Ne/DME mixture. The anode HV value at which the four measurements were made has been chosen to be about 50 V above the knee of the HV efficiency curve for each gas mixture (Figure 3). All the distributions have been fitted with a skewed gaussian function of the form:

$$y = P_1 \exp\left(-\frac{1}{2} \frac{(x - P_2)^2}{P_3 - P_4(x - P_2)^2}\right).$$

C. Position Resolution

We first discuss the position resolution measured with the 400 μm pitch chambers and later with the 200 μm pitch. The resolution is first measured using the 3 point technique. Cathode hits were found in a telescope of three identical MSGCs for high statistics runs taken on the plateau of the efficiency curve. A straight line is drawn between the hits of the 2 outside detectors predicting a hit in the middle chamber. We then generate, for the middle chamber, the distribution of residuals of the track's position in this chamber with the found hit. This plot is expected to show a gaussian shape, whose sigma is related to the resolution of the three MSGCs. Figure 6a) gives such a distribution measured with MSGCs with a substrate of glass S-8900, 7 mm thick, and operated with 100% DME gas. When a gaussian function is fit to the data in the range of -2σ to 2σ , the observed sigma is 81 μm . To calculate the resolution from this number, one must first subtract the contribution of the multiple scattering and then apply a factor $\sqrt{2/3}$ to account for the resolution of the

two outside detectors (assuming the three MSGCs have the same resolution and the errors are not correlated). The contribution of multiple scattering, calculated with a GEANT Monte Carlo, is $21 \mu\text{m}$. After these corrections the position resolution, for the $400 \mu\text{m}$ pitch chamber, is calculated to be $64 \mu\text{m}$.

To improve this result, we look at the scatter plot (Figure 7a)) of the position of the extrapolated tracks in the middle detector (vertical axis) versus the position of the centroid (horizontal scale) in the same chamber. This scatter plot superimposes the information of many cathodes over a distance of one pitch interval ($\pm 0.2 \text{ mm}$). In this plot the origin of the axis is the center of the anode. Rather than observing a continuous band of points along a 45° line, the data follow an s-shaped curve. This suggests that there is a systematic bias in the reconstructed centroid relative to the true position of the hit. We use an empirically derived function to correct this bias, with the distance of the centroid from the nearest anode as the independent variable. In deriving this function we must consider the effect of the similar bias in the chambers used to define the track. We account for this by iterating our correction function. That is, we apply the correction function to the outer chambers and compute a new bias for the middle MSGC. Because the geometry makes this bias in the outer chambers relatively unimportant, this procedure quickly converges to a stable function. Figure 7a) shows superimposed to the scatter plot the profile histograms (average of data binned along the horizontal scale) of the measurements (diamonds) as well as the function that best fits the data. The fitted function and the best fit parameters are given in the figure caption. Figure 8a) is the histogram of the data shown in Figure 7a). They show a strong clustering of the data at the position of the anode, rather than a uniform distribution. After applying to the centroids the correcting function, the scatter plot of Figure 7a) is transformed into Figure 7b) which shows a distribution around a 45° line. The histogram in Figure 8b) shows how the now corrected centroids fill the interval of size one pitch more uniformly. The resulting distributions of residuals is plotted in Figure 6b). A gaussian fit in the range of -2σ to 2σ to the distribution with corrected hits has a sigma of $56 \mu\text{m}$. After subtracting the contribution due to multiple scattering and applying the factor $\sqrt{2/3}$, we obtain a position resolution of $42 \mu\text{m}$ for a $400 \mu\text{m}$ pitch MSGC.

The data from the $200 \mu\text{m}$ pitch region of the MSGC's, give a resolution of $45 \mu\text{m}$ using uncorrected centroids after subtracting the multiple scattering and including the factor $\sqrt{2/3}$ (Figure 9a). Applying the same correction procedure as discussed above one obtains (Figure 10, and 11) a position resolution of $42 \mu\text{m}$ (Figure 9b). We estimate the uncertainty on these resolutions at $\pm 2 \mu\text{m}$ based on the re-analysis of the data with different selection criteria and fitting methods.

The major limitations of this analysis are related to the relatively large noise of

the available preamplifiers. In order to derive the correction function, fiducial cuts were applied to remove the regions of the telescope where any one of the three chambers did not operate normally. The interpolation technique is applicable only in the case that the signal to noise is such that most clusters contain at least two cathodes. It is expected that a fully efficient chamber would always contain at least two cathode channels per cluster. By using preamplifiers with lower noise than the ones used for the present measurement, one should be able to achieve the same resolution at lower gas gain. As a test, we have checked the resolution improvement achieved with our technique on a run taken at a lower voltage and found a comparable improvement when single cathode clusters are disregarded.

A previous analysis of data from a 200 μm pitch MSGC using the information of the cathodes [9] [21], has utilized similar corrections but the improvement in resolution was not discussed. However, our results are in agreement with the conclusions presented in that work.

We think that the considerable improvement achieved in the position resolution of MSGCs with large pitch and using the information of the cathodes can be explained by assuming that the development of the avalanche depends on the angle at which the electrons are drifting when the avalanche forms. In the drift field of a MSGC this angle is correlated to the distance of the track from the anode. The avalanche reflects this information which can then be extracted from the signals induced in the cathodes to calculate a correcting function. In the case of a MWPC the fact that the avalanche does not develop uniformly around the anode is well documented and it has been suggested to exploit this for resolving left right ambiguities in drift chambers [22] – [24]. To our knowledge this is the first time that a substantial improvement of the position resolution has been achieved by using the pulse height information of the cathodes strips in MSGC. Similar analysis [25] – [28] have been made for different physical cases, where cathode strips have been used to determine a coordinate along the wires of MWPCs.

D. Time Resolution

The time resolution of the MSGCs signals has been measured using a TDC (LRS 2228A). The anodes signals (corresponding to groups of 4 channels) for the 400 μm region of one MSGC were split such that one of the signals was analyzed by the ADCs and the other was first amplified (LRS621A), then discriminated (LRS620B) at 20 mV and its time measured relative to the triple coincidence of scintillator counters. Data were taken using a gas mixture of Ne/DME (14/86) and with pure DME. Figure 12 shows the combined time distribution for all the channels of one MSGC for hits on a track. The data,

which has been corrected for small variations in the length of the readout chain, shows a gaussian peak and tails associated with the smaller signals. The time distribution for the mixture of Ne/DME is slightly narrower than for pure DME. The r.m.s. values are quoted in the figure. The fraction of the events contained in a time interval of 25 ns is 92% for events collected with Ne/DME gas and 90% for the pure DME data. This time resolution is consistent with previously published values [29].

IV. Monte Carlo Studies

We have developed a two part Monte Carlo simulation of the MSGC to estimate the two track separation as well as the position resolution for tracks not at normal incidence. In the first part of the simulation the BNL test configurations are placed into GEANT. In this step the errors due to multiple scattering and geometry are accounted for. In the next step an algorithm generates a charge distribution in the detector and then deposits the charge onto the MSGCs' electrodes. The charge is generated according to fitted Landau distributions of clusters measured with the cathodes in a MSGC operated with 100% DME. The simulated charge distribution has been normalized to the observed single channel pedestal widths, thus defined in S/N units. This charge is then randomly distributed along a number of points of the trajectory, corresponding to the expected number of ionization electrons per cm. The spreading of the charge transverse to the trajectory depends on diffusion and delta rays and it is described by a gaussian distribution whose sigma of 100 μm was chosen to reproduce the observed cluster multiplicity. The derived number for the sigma of the charge spread is consistent with measured diffusion coefficients. The charge, is then projected onto cells with width equal to the pitch of the MSGC and the single channel pedestal noise is added. This model would better represent the case where the anode signals are read out. From this information, clusters are identified by an algorithm which requires clustered channels to be within ± 5 channels of a maximum and each channel in the cluster to be 3 sigma above the pedestal.

The efficiency for two-track separation was studied by generating pairs of clusters at a known distance apart and reconstructing the centroids as before. As the clusters are brought closer together the centroids become ambiguous and the two-track resolution is lost. We define the efficiency of reconstruction of double clusters as the fraction of events in which both centroids are reconstructed and whose residuals falls within 2 sigma of the one cluster residual. A double cluster finding efficiency of 95% is achieved for separations of 450 μm and 875 μm in the 200 and 400 μm respectively.

With the same Monte Carlo we study the effect of the position resolution for

tracks not at normal incidence. In general, the resolution deteriorates strongly for non-normal incidence. The results of the simulation show that at an angle of 25° the resolution of $400\ \mu\text{m}$ pitch chambers is $100\ \mu\text{m}$, a factor of two better than that of $200\ \mu\text{m}$ pitch.

V. Potential Applications

Reading out the cathodes offers a number of options in the application of MSGCs. For instance, if the S/N is large enough, the rectangular cathode pad can be subdivided into triangular shapes and from the information of both sections the coordinate along the electrodes can be derived. The MSGC then becomes a 2D device. Another possibility is to segment the cathodes along their length. The signal from each element is carried across the substrate with plated through hole to a preamplifier and the MSGC becomes a pixel device. The improvement in position resolution, achieved using the described correcting function, can also be applied to the Micro Gap Chamber and in this case too the number of readout channels could be substantially reduced.

VI. Summary

We give here a list of our major results.

- Position resolutions of the order of $40\ \mu\text{m}$ have been achieved utilizing the cathodes readout information of MSGCs with a pitch of $400\ \mu\text{m}$ (similar to values obtained with $200\ \mu\text{m}$ pitch chambers). This is possible after correcting the centroid of the cluster with a function derived from the data.
- The time resolution of the anode signals from MSGCs with $400\ \mu\text{m}$ pitch and operated with 100% DME had an r.m.s of 14 ns (and 16 ns for Ne/DME). An interval of 25 ns includes 92% (100% DME) of the events (90% for Ne/DME)
- MSGCs with a $400\ \mu\text{m}$ pitch reach full efficiency well before reaching break down and their operation is much more reliable than for the $200\ \mu\text{m}$ pitch ones.
- Our data show that 8 bit ADC resolution is sufficient to apply the interpolating technique used with our data to achieve a position resolution of about $40\ \mu\text{m}$.
- A simple Monte Carlo calculation confirms the expectation that the angular dependence of the position resolution is less pronounced (by a factor of 2) in the $400\ \mu\text{m}$ pitch than in the $200\ \mu\text{m}$.

- Given the dependence of the resolution of MSGCs with 200 μm pitch on the angle of incidence of the tracks the commonly quoted value of the resolution at normal incidence may not be the most appropriate quantity when describing tracking with MSGCs for a specific experiment. More significant could be an average resolution which accounts for the geometry of the particular experiment and for the angular dependence of the resolution in MSGCs. If the occupancy does not require the smallest possible pitch of the chambers, one could obtain the same overall position resolution with half the number of readout channels. This also has important economic implications for large detectors.

VII. Acknowledgments

We acknowledge the help received from Brookhaven National Laboratory and in particular from Dr. Alan Carroll, David Dayton and the Printed Circuit Laboratory. Fermilab has generously allowed us to use its facilities and the Physics Dept. MicroDetector Group has played an essential role. The DØ project at Fermilab has made available some of the readout electronics, its staff has contributed significantly, and especially the help received from Delmar Miller has been greatly appreciated. We thank Fabio Sauli for numerous illuminating discussions. Research grants from DOE and NSF to the participating institutions have made this work possible.

-
- [1] A. Oed, *Nucl. Instr. and Meth.* **A263** (1988) 351-359.
 - [2] F. Hartjes et al., *Nucl. Instr. and Meth.* **A310** (1991) 88-94.
 - [3] F. Sauli, Development of the Micro-Strip Gas Chambers for Radiation Detection and Tracking at High Rates, *CERN/DRDC/92-93, 93-34, 94-45*.
 - [4] R. Bouclier et al., *Nucl. Instr. and Meth.* **A367** (1995) 168-172.
 - [5] O. Bouhali et al., *Preprint IISN0379-301X*, Feb. 1996, (Submitted to *Nucl. Instr. and Meth.*)
 - [6] T. McMahan et al., *Nucl. Instr. and Meth.* **A348** (1994) 361-364.
 - [7] M.S. Dixit et al., Proceedings of the International Workshop on Micro-Strip Gas Chambers, Legnaro, October 13-14, 1994, p138, Editors: G. Della Mea, F. Sauli.
 - [8] F. Angelini et al., *Nucl. Instr. and Meth.* **A360** (1995) 22-29.
 - [9] R. Bouclier et al., *Nucl. Instr. and Meth.* **A367** (1995) 163-167.
 - [10] O. Adriani et al., *Nucl. Instr. and Meth.* **A367** (1995) 189-192.
 - [11] F. Angelini et al., *Nucl. Instr. and Meth.* **A368** (1996) 345-352.
 - [12] N. Amos et al., Proceedings of the International Workshop on Micro-Strip Gas Chambers, Lyon, Nov. 30 - Dec. 2, 1995, Editors: D. Contardo and F. Sauli.

- [13] A. Angelini, et al., *Nucl. Instr. and Meth.* **A315** (1992) 21-32.
- [14] F. Udo (NIKHEF), Hermes experiment at DESY., Private Communication.
- [15] The Compact Muon Solenoid, Technical Proposal, *CERN/LHCC 94-38 LHCC/P1*, (December 1994).
- [16] R. Bouclier et al., *Nucl. Instr. and Meth.* **A350** (1994) 464-469.
- [17] IMT, Masken and Teilungen AG, Im Langacher, CH-8606 Greifensee.
- [18] Fujipoly Inc., 750 Walnut Ave. Cranford, NJ 07016, USA.
- [19] R.J. Yarema, *IEEE Trans. Nucl. Sci.* **NS33** (1986) 933 (MB43458).
- [20] R. Bellazzini (INFN Pisa), Private communication.
- [21] M. Capeans, Ph.D. Thesis, Study of the Ageing of Gaseous Detectors and Solutions for the Use of MSGCs in High Rate Experiments, Universidad de Santiago de Compostela.
- [22] A.H. Walenta, *Nucl. Instr. and Meth.* **151** (1978) 461-472.
- [23] A. Breskin et al., *Nucl. Instr. and Meth.* **151** (1978) 473-476.
- [24] G. Charpak et al., *Nucl. Instr. and Meth.* **162** (1979) 405-428.
- [25] G. Charpak et al., *Nucl. Instr. and Meth.* **167** (1979) 455-464.
- [26] F. Piuz et al., *Nucl. Instr. and Meth.* **196** (1982) 451-462.
- [27] J.Chiba et al., *Nucl. Instr. and Meth.* **206** (1983) 451-463.
- [28] G. Bencze et al., *Nucl. Instr. and Meth.* **A357** (1995) 40-54.
- [29] J.F. Cleargeau et.al., Proceedings of the International Workshop on Micro-Strip Gas Chambers, Legnaro, October 13-14, 1994, p64 Editors: G. Della Mea, F. Sauli.

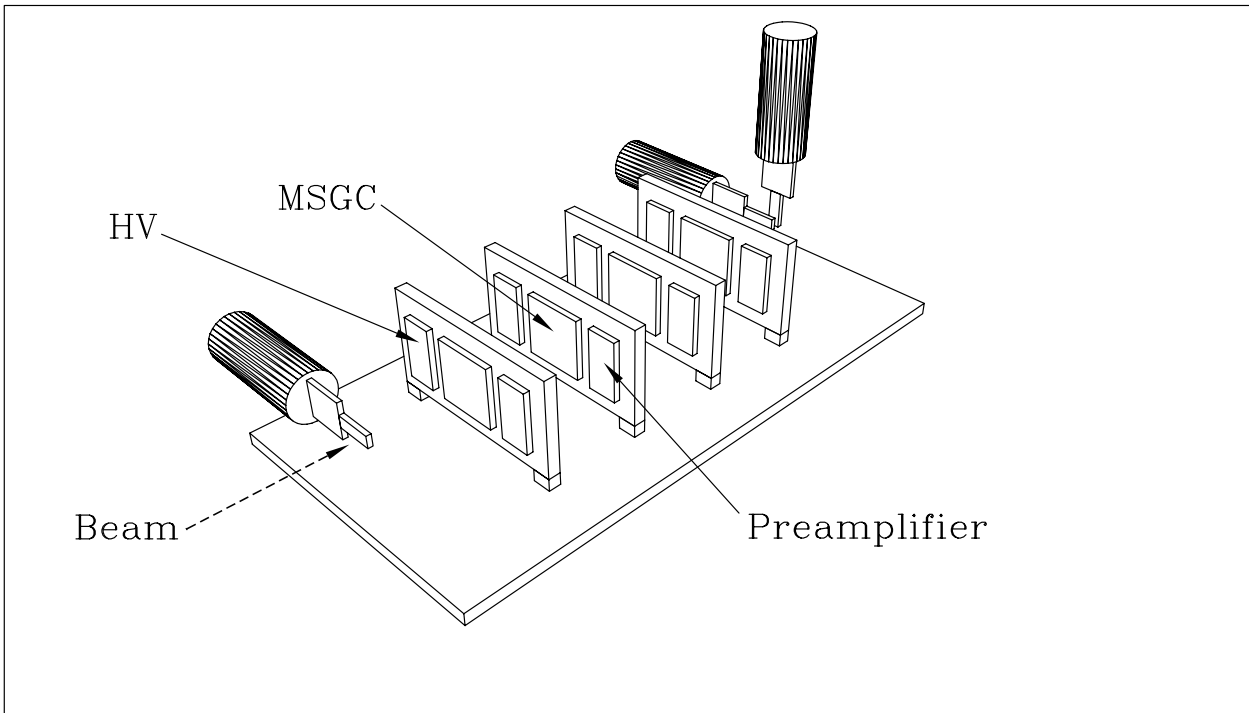


FIG. 1. The experimental setup used at the BNL testbeam.

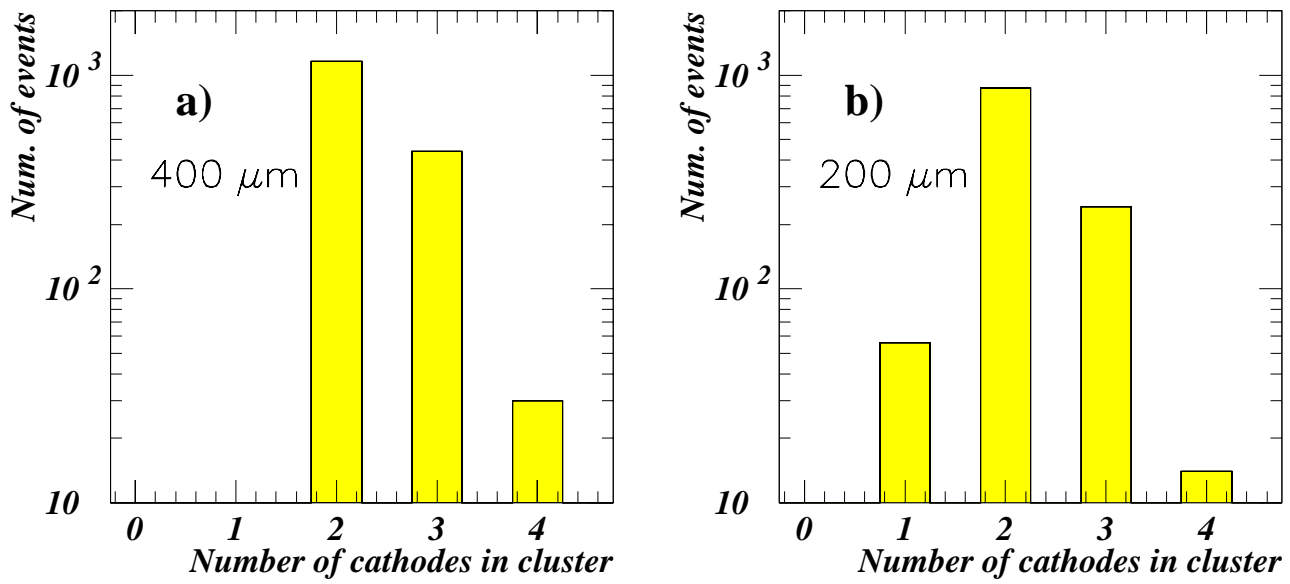


FIG. 2. Distribution of cluster multiplicities. a) 400 μm pitch (HV= -2400 V/+760 V, 100% DME, S-8900) b) 200 μm pitch (HV= -2400 V/+820 V, 100% DME, S-8900)

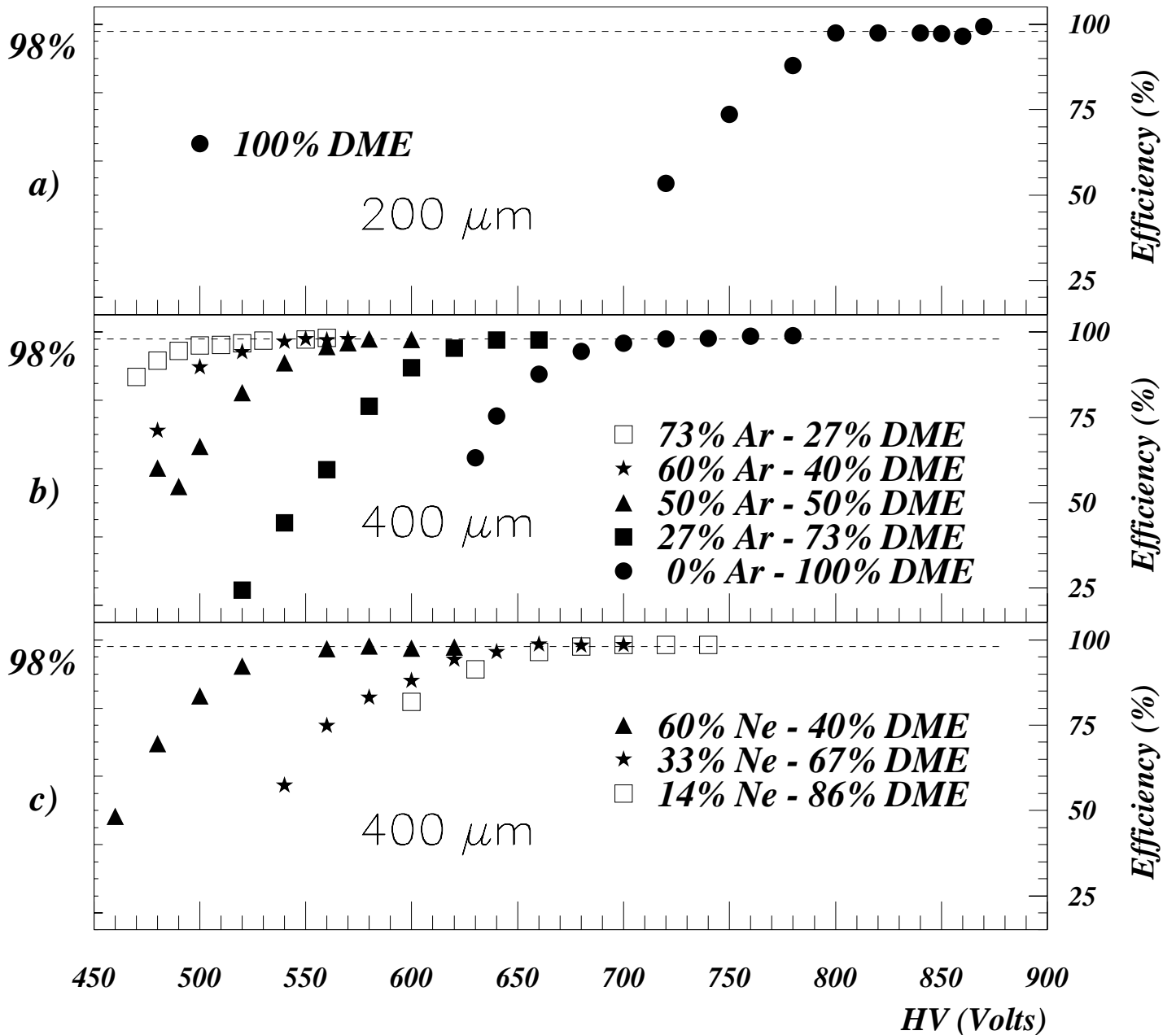


FIG. 3. Efficiency curves for MSGCs for different gasses. a) 200 μm pitch (drift HV = -2000 V, 100% DME, D-263) b) 400 μm pitch (drift HV = -2000 V, various mixtures of Ar and DME, D-263) c) 400 μm pitch (drift HV = -2000 V, various mixtures of Ne and DME, D-263)

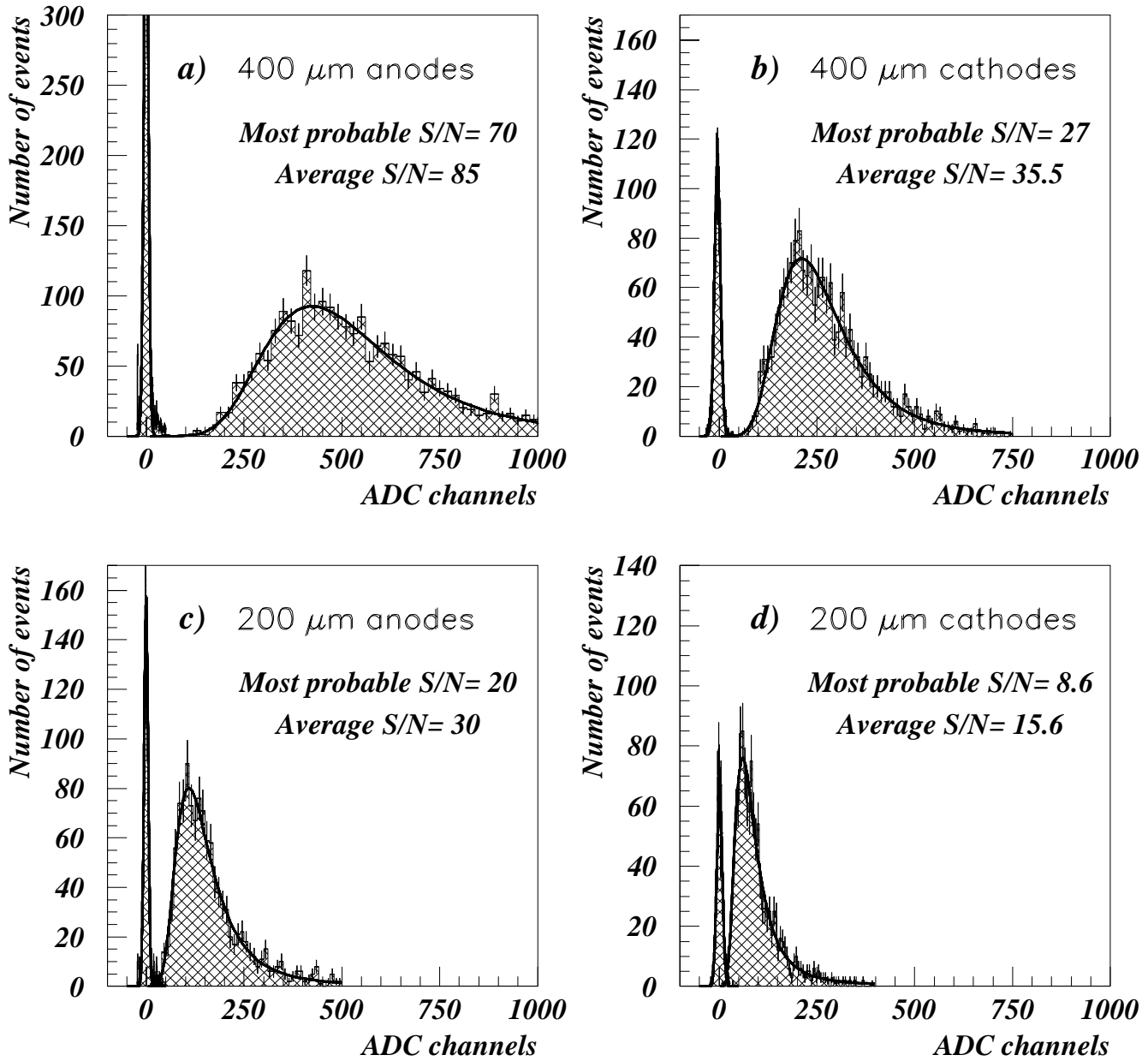


FIG. 4. Signal and pedestal distribution measured with an MSGC (S-8900) operated with 100% DME. a) 400 μm pitch anodes (HV= -2400 V/+760 V) b) 400 μm pitch cathodes (HV= -2400 V/+760 V) c) 200 μm pitch anodes (HV= -2400 V/+820 V) d) 200 μm pitch cathodes (HV= -2400 V/+820 V)

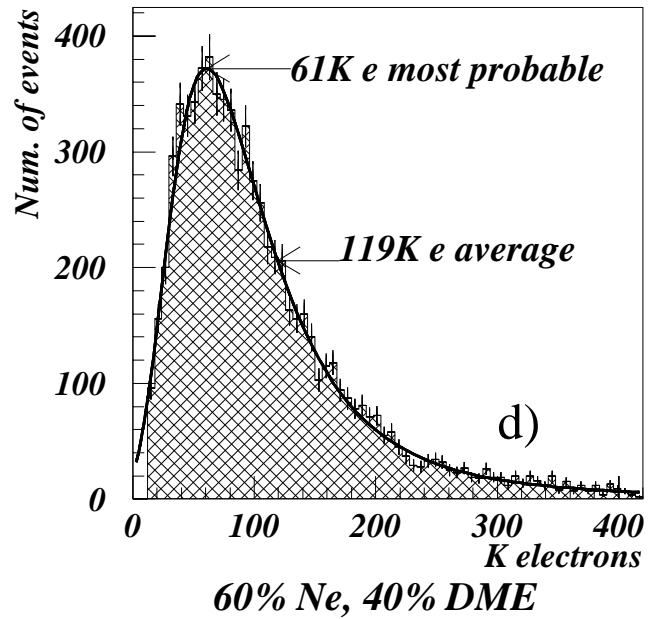
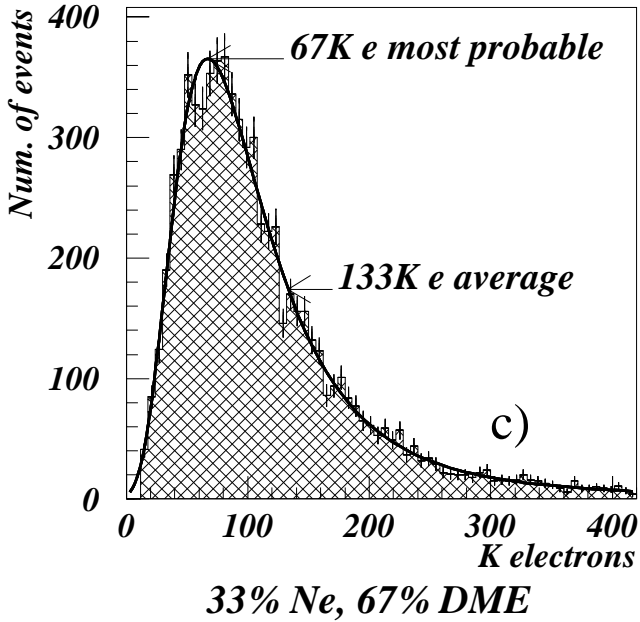
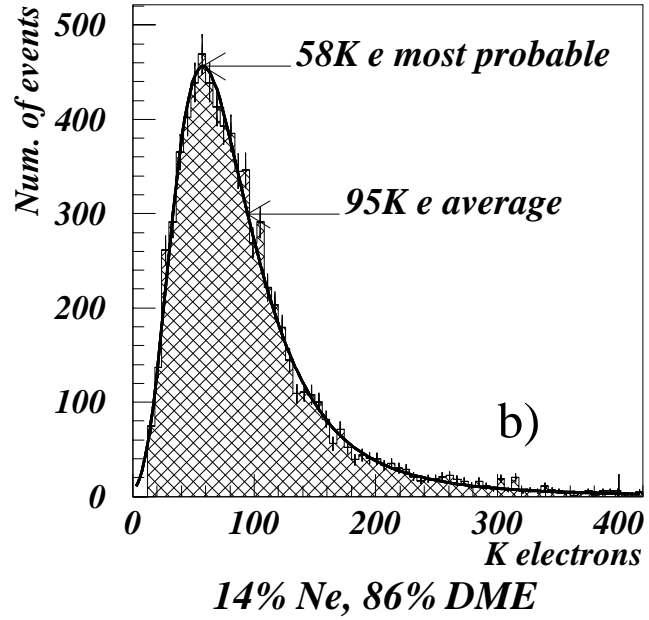
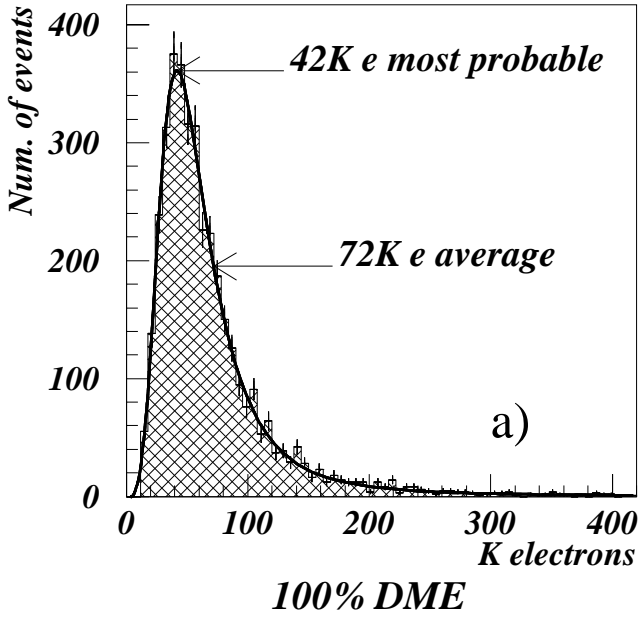


FIG. 5. Pulse height distribution measured with the anodes on D-263 substrate for various mixtures of Ne and DME. The drift HV was -2000 V, and the anode HV a) 700 V, b) 680 V, c) 640 V, d) 560 V.

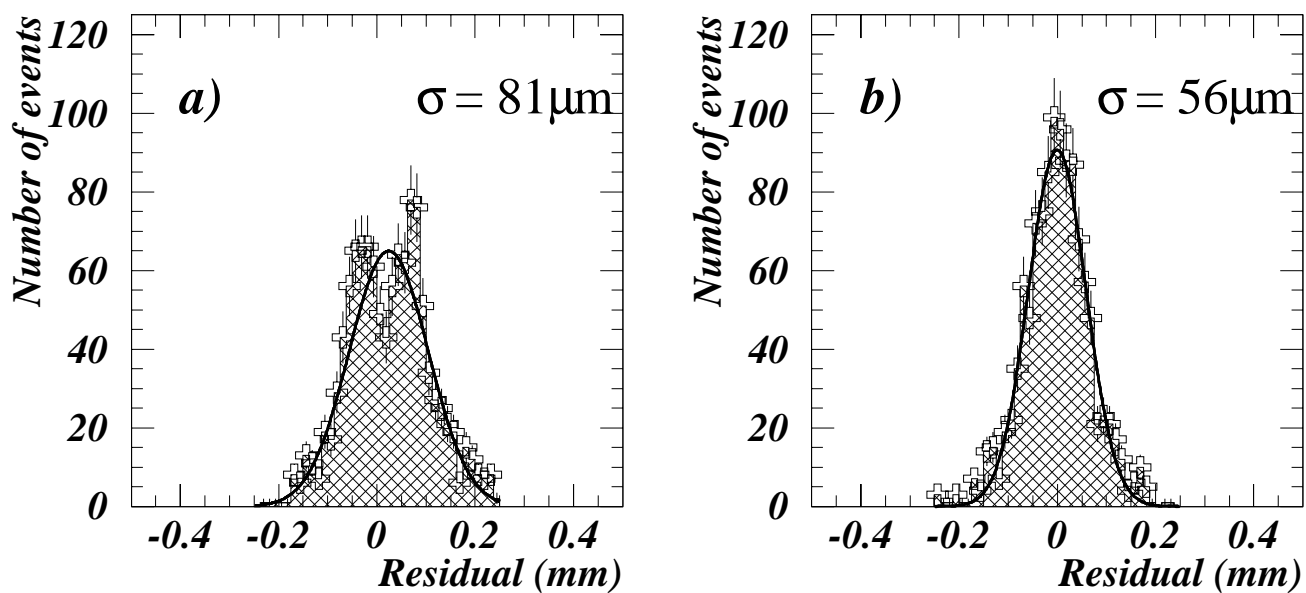


FIG. 6. Distribution of residuals measured with a $400\ \mu\text{m}$ pitch substrate before corrections (a) and after corrections (b). (HV= -2400 V/+760 V, 100% DME, S-8900). Cathode readout is used. No corrections are applied for multiple scattering or the resolution of the beam defining chambers.

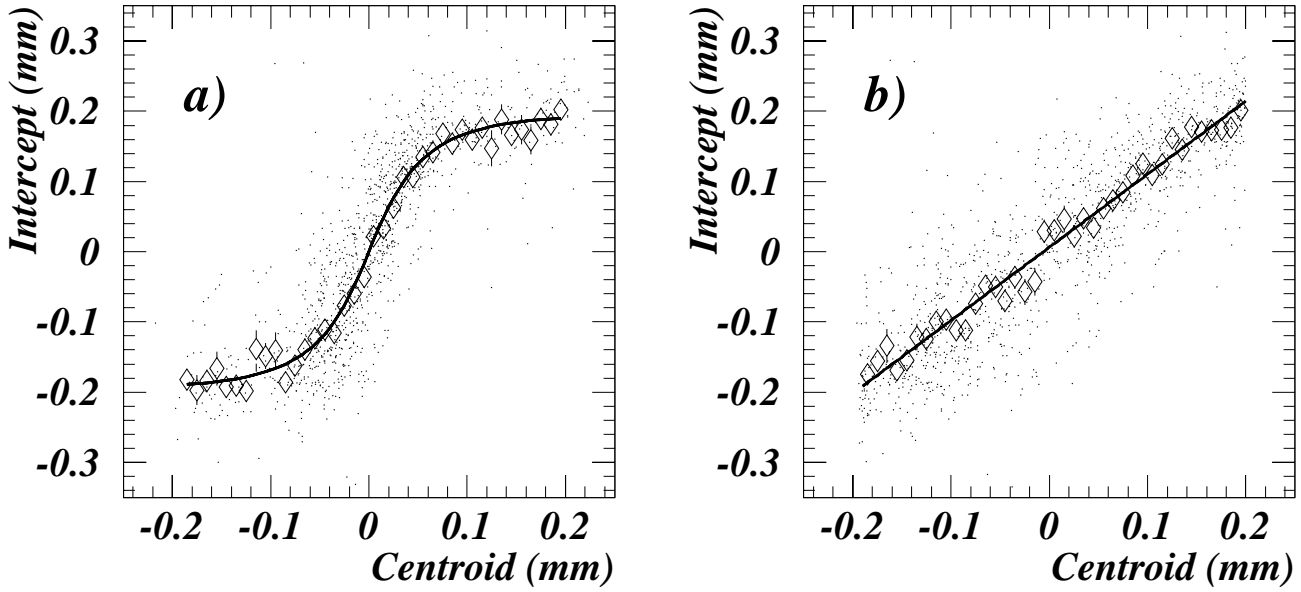


FIG. 7. Scatter plot of the track intercept versus the cluster centroid for the 400 μm before corrections (a) and after corrections (b). The position is plotted as the distance from the nearest anode. The diamond symbols are the profile histogram. The correction function is also drawn in figure a). $f(x) = p_1 \cdot x + p_2 \cdot \arctan(p_3 \cdot x)$. The parameters are found by χ^2 minimization to be as follows: $p_1 = -.09\text{mm}$, $p_2 = .15\text{mm}^{-1}$, $p_3 = 22$. In figure b) a straight line fit to the corrected data gives $\chi^2/\text{ndf} = 2.2$

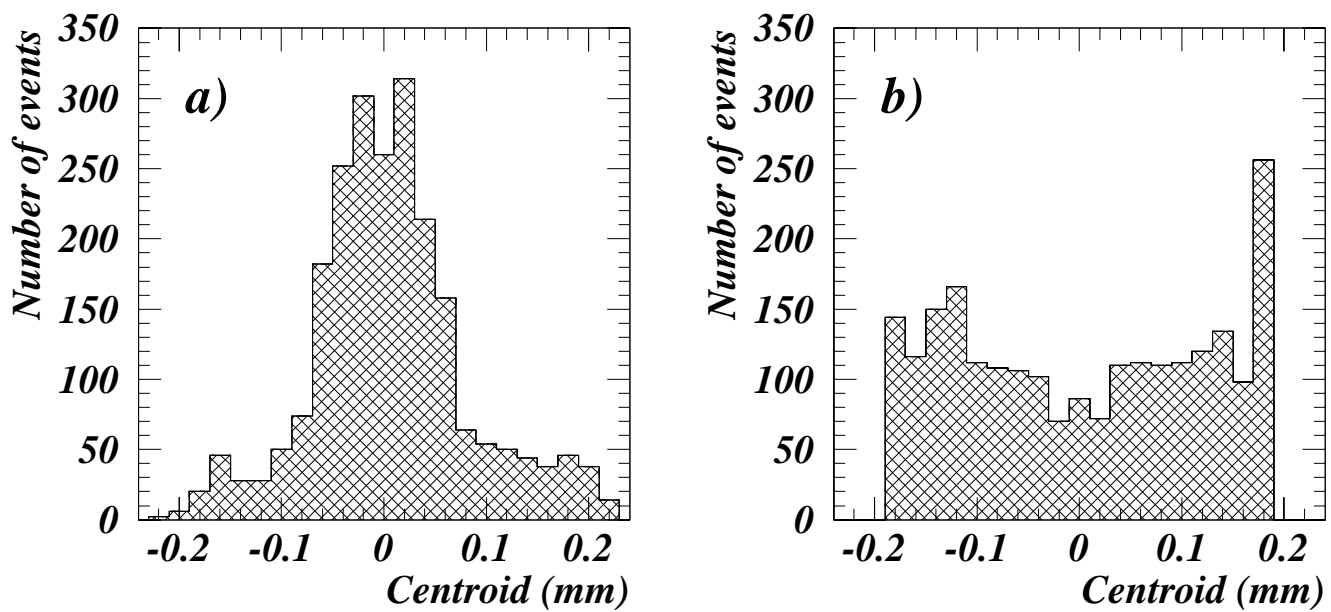


FIG. 8. Histogram of the centroid in the middle chamber as a function of the distance from the nearest anode, shown before corrections (a) and after corrections (b). (Same data as in Figure 6.)

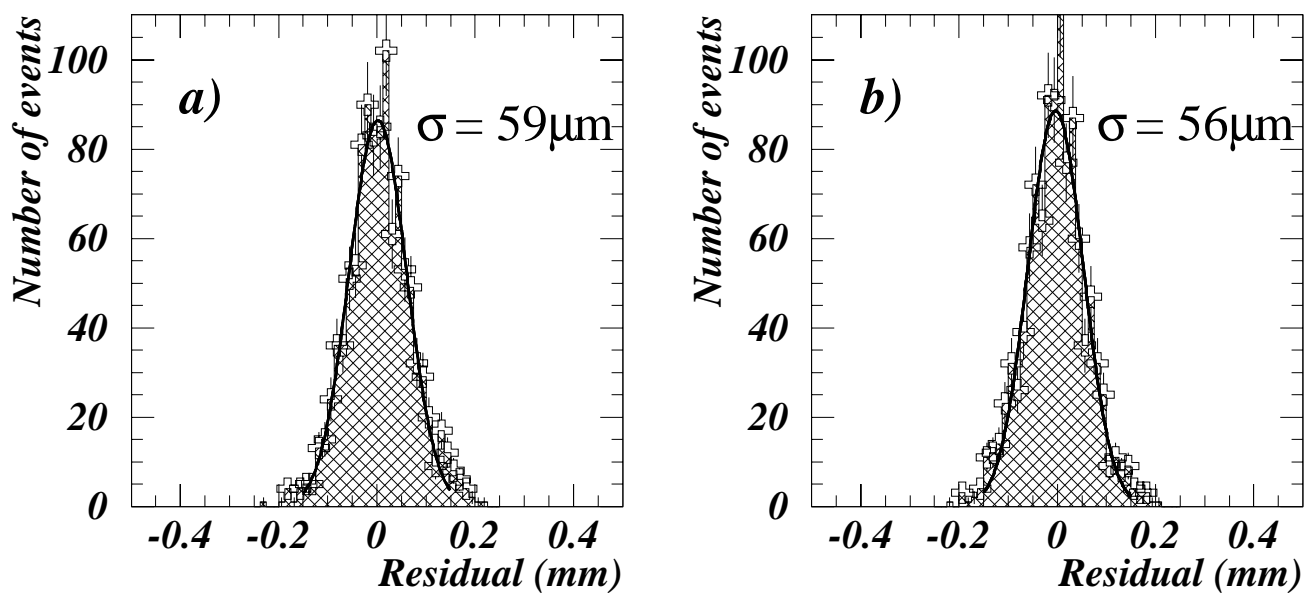


FIG. 9. Distribution of residuals measured with a $200\ \mu\text{m}$ pitch substrate before corrections (a) and after corrections (b). (HV= -2400 V/+820 V, 100% DME, S-8900). Cathode readout is used. No corrections are applied for multiple scattering or the resolution of the beam defining chambers.

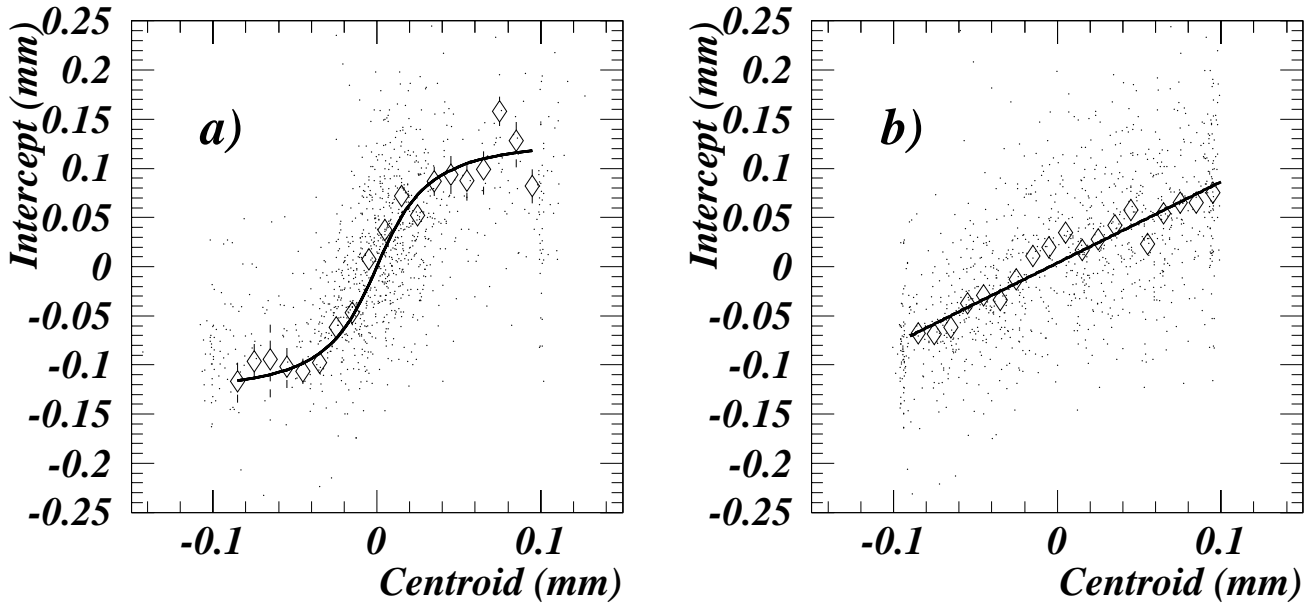


FIG. 10. Scatter plot of the track intercept versus the cluster centroid before corrections (a) and after corrections (b) for the 200 μm pitch. The position is plotted as the distance from the nearest anode. The diamond symbols are the profile histogram. The correction function is also drawn in figure a). The function has the same form as for the 400 μm pitch: $f(x) = p_1 \cdot x + p_2 \cdot \arctan(p_3 \cdot x)$. The parameters are found by χ^2 minimization to be as follows: $p_1 = -.05\text{mm}$, $p_2 = .075\text{mm}^{-1}$, $p_3 = 41$. In figure b) a straight line fit to the corrected data gives $\chi^2/\text{ndf} = 2.3$

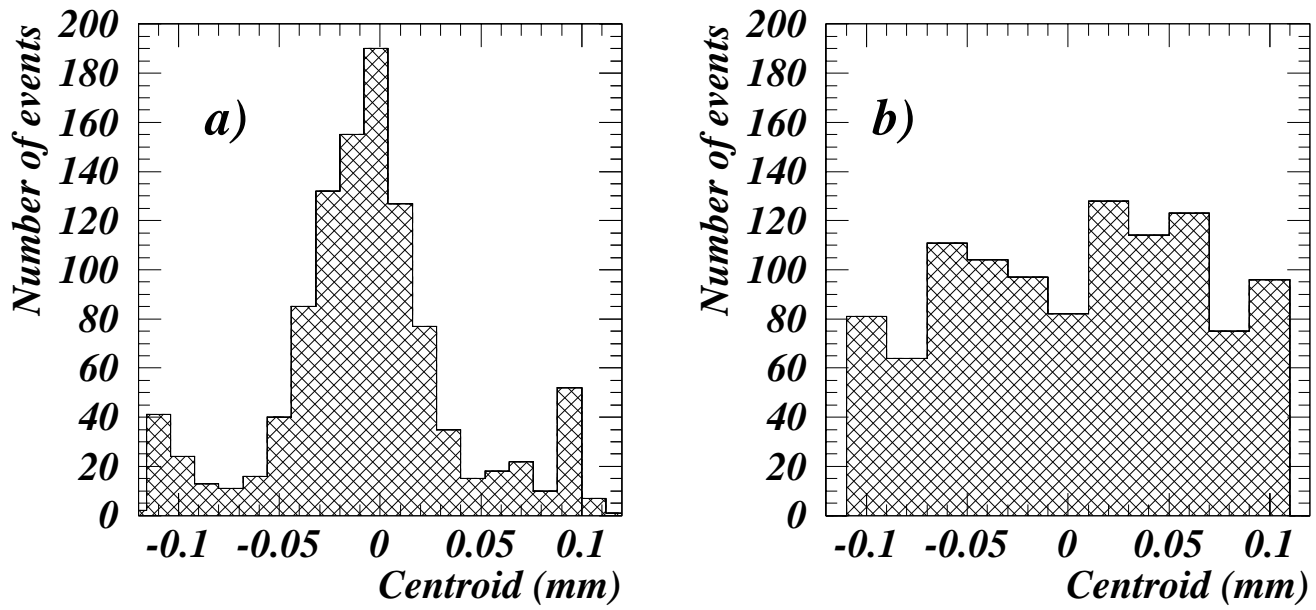


FIG. 11. Same as Figure 8 but for the 200 μm pitch section.

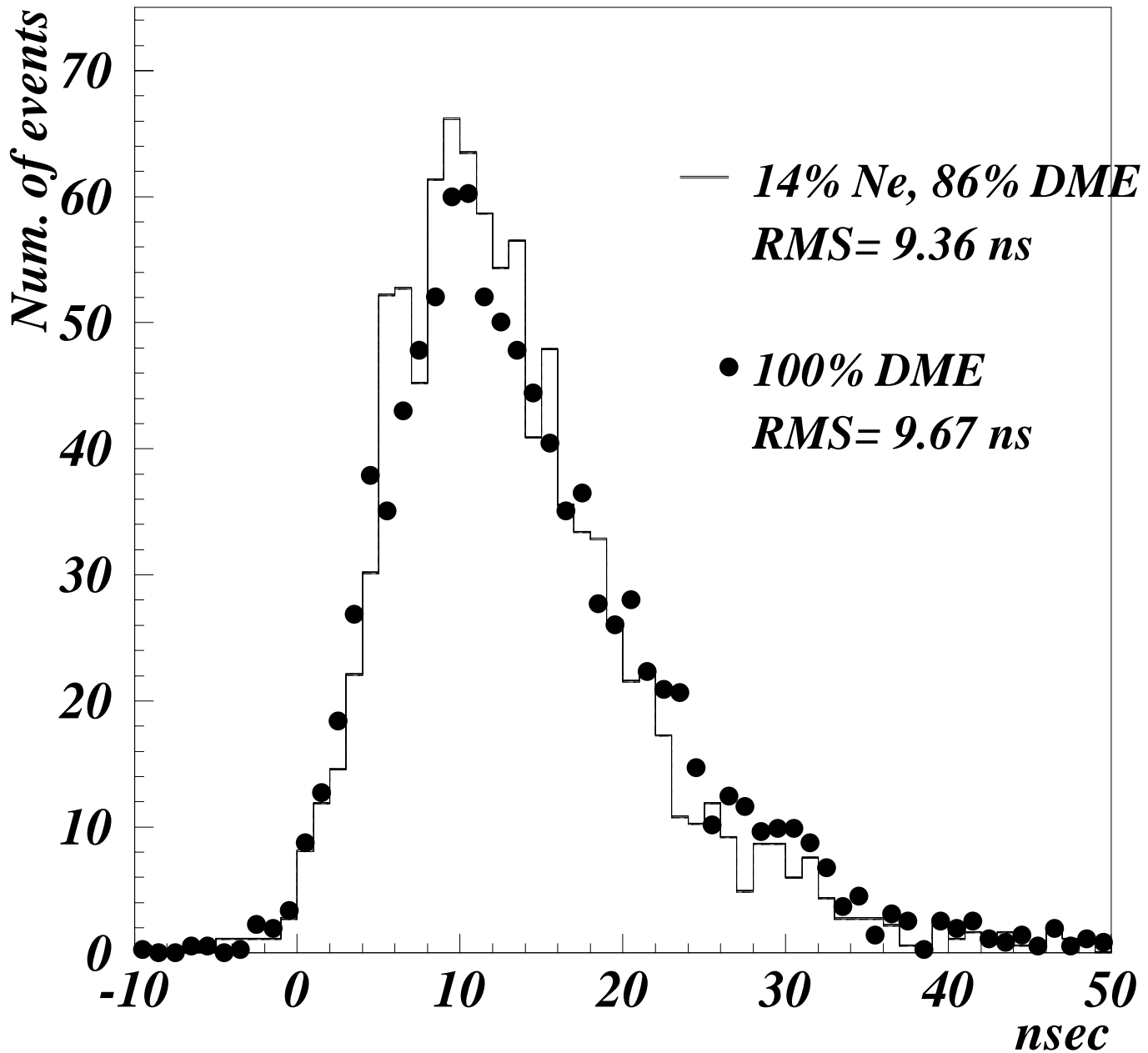


FIG. 12. Time distribution of signals above 20 mV for 400 μm pitch anodes for pure DME (D-263, HV= -2400 V/+760 V) and a mixture of Ne and DME (D-263, HV= -2400 V/+730 V).